

On the Closure of the Scalar Dissipation Rate in the Spray Flamelet Equations

H. Olguin^{1*}, A. Scholtissek², S. Gonzalez¹, F. Gonzalez¹, M. Ihme³, C. Hasse², E. Gutheil⁴

¹Department of Mechanical Engineering, Universidad Técnica Federico Santa María, Avenida España 1680, Valparaíso, Chile

²Institute for Simulation of Reactive Thermo-Fluid Systems, TU Darmstadt, Otto-Berndt-Straße 2, 64287 Darmstadt, Germany

³Department of Mechanical Engineering, Stanford University, Stanford, CA 94305, USA

⁴Interdisciplinary Center for Scientific Computing, Heidelberg University, Im Neuenheimer Feld 205, 69120 Heidelberg, Germany

*Corresponding author: hernan.olguin@usm.cl

Abstract

In this paper, closure of the Scalar Dissipation Rate (SDR) in the Spray Flamelet Equations (SFE) is addressed. For this purpose, the gradient g_ξ of the mixture fraction ξ is used instead of the SDR itself. A transport equation for g_ξ is derived and transformed from physical into mixture fraction space. Moreover, the SFE of the species mass fractions and of gas temperature are re-derived in terms of g_ξ for consistency, where differential diffusion is considered. In the resulting set of equations, two different kinds of unclosed quantities appear: source terms due to momentum and energy exchange between the liquid phase and the gas phase and the spatial gradient of the product of the gas velocity and the gas density, $\hat{a} = d(\rho u_y)/dy$. Closure of the latter is the focus of the present study. Numerical simulations of different counterflow ethanol/air flames in physical space are carried out using a well established detailed model, and the results are employed for the validation and analysis of the newly proposed set of SFE. In particular, a non-premixed gas flame is established as a base case and then perturbed by means of different mono-disperse sprays injected from the air side of the configuration. Introducing a stream-like function, an expression for \hat{a} is obtained. The validation confirms that the new set of SFE perfectly reproduces the counterflow structure when the correct profiles of the unclosed evaporation-related source terms are available. Moreover, the suitability of imposing a constant value for the closure of \hat{a} is tested in terms of the ability of the SFE of properly predicting both g_ξ and the spray flamelet structure of the reference counterflow flames. Two different alternatives are considered for the constant value of \hat{a} : its value at the location of stoichiometric mixture fraction and its value at the air side of the counterflow configuration. The contributions of the individual terms in the SFE are analyzed, providing insight into the influence of evaporation. It is found that the main physical phenomena in the counterflow (spray) flames are adequately recovered when the value of \hat{a} at stoichiometric mixture is employed. The proposed approach provides advancement towards the development of a comprehensive and self-contained spray flamelet theory.

Keywords

Spray Flamelet Equations, Scalar Dissipation Rate, Counterflow Flames

Introduction

Following the classical work of Peters [1], a non-premixed flamelet can be defined as an essentially one-dimensional structure located in the reaction zone of a thin flame. This assumption is formally introduced by a change of coordinates of the conservation equations of species mass fractions and energy from the three-dimensional physical space, (\vec{x}, t) , into a one-dimensional composition space, (ξ, τ) , where ξ is the mixture fraction and τ is a time-like variable [1]. This procedure is well established for non-premixed gas flames. In the transformed set of equations, the so-called (gas) flamelet equations, the only unclosed variable is the Scalar Dissipation Rate (SDR), χ . The flamelet equations can be closed in composition space using either the complementary error function (erfc) or the natural logarithm (ln) for modeling the SDR [1]. For spray flames, studies focussing on the Spray Flamelet Equations (SFE) in mixture fraction space have appeared only very recently [2, 3, 4, 5]. In these much more complex flames, there is a need for appropriate models for the closure of the scalar dissipation rate and the evaporation-related source terms appearing in the SFE, being the former the main objective of the present work.

The inherent difficulties associated with the obtention of general analytical profiles of the SDR increase the attractiveness of approaches directly considering a transport equation for the scalar dissipation rate χ in composition space [6, 7], since they may take into account any arbitrarily complex evaporation profile. However, even though transport equations for the SDR in spray flames in physical space have been proposed in recent years [4, 8], no attempt has yet been made to implement them for closure of the SFE, which is attributable to their complexity and the expected stiffness of the resulting set of equations. Recent work of Scholtissek et al. [9] suggests that considering the gradient of the mixture fraction instead of the SDR could lead to a solvable and easy to handle system. This alternative will be explored in the present paper.

Thus, a transport equation for the gradient of the mixture fraction, $g_\xi(\xi)$ is derived and evaluated. For consistency, the spray flamelet equations for the species mass fractions and for gas temperature will be re-derived in terms of

this variable. The newly proposed set of SFE will be validated in the context of three laminar ethanol/air counterflow flame structures generated with a well established approach [10, 11]. Specifically, an ethanol/air gas flame in which an air stream is injected from the left side of the configuration and directed against a pure fuel stream will be established as a base case and perturbed by injecting two different mono-disperse sprays from the air side of the configuration. Introducing a stream-like function, an expression for the gas velocity in mixture fraction space will be derived from the global mass and momentum balance equations and used then for closure of the gradient of the product of the gas density ρ and the axial gas velocity u_y , $\hat{a} = d(\rho u_y)/dy$. Moreover, the appropriateness of imposing a constant value for the closure of \hat{a} will be tested in terms of the ability of the SFE of properly predicting both g_ξ and the spray flamelet structure of the reference counterflow flames. Two different alternatives will be considered for the constant value of this quantity: its value at the stoichiometric point and its value at the air side of the counterflow configuration. Particular emphasis will be given to the budget of the different terms of the spray flamelet equations, which will be studied to determine whether the main physical phenomena taking place in these flames are properly predicted and how evaporation affects the quality of the assumptions. The results intend to provide advancement towards the formulation of a comprehensive and self-contained spray flamelet theory.

Governing Equations

For steady, axi-symmetric dilute counterflow spray flames, the governing equations for total mass and momentum in the radial direction can be written as [10, 11]

$$\frac{1}{r} \frac{\partial(\rho u_r r)}{\partial r} + \frac{\partial(\rho u_y)}{\partial y} = \dot{S}_v \quad (1)$$

and

$$\rho u_r \frac{\partial u_r}{\partial r} + \rho u_y \frac{\partial u_r}{\partial y} = -\frac{dp}{dr} + \frac{\partial}{\partial y} \left(\mu \frac{\partial u_r}{\partial y} \right) + \dot{S}_m, \quad (2)$$

respectively, where the boundary layer approximation has been adopted and low Mach number has been assumed [10]. In these equations, ρ is the gas density, u_r and u_y are the radial and axial gas velocity, respectively, μ is the dynamic gas viscosity and \dot{S}_v and \dot{S}_m are sources due to the exchange of mass and momentum between the liquid and the gas, respectively. Moreover, a similarity transformation allows transferring the two-dimensional gas equations for the mass fractions Y_k ; $k = 1, \dots, N$ of chemical species k and of gas temperature into a one-dimensional formulation [10, 11]. This yields

$$\rho u_y \frac{dY_k}{dy} = -\frac{d(\rho V_{ky} Y_k)}{dy} + \dot{\omega}_k + \dot{S}_v (\delta_{kF} - Y_k). \quad (3)$$

The term including the diffusion velocity is calculated as

$$\rho V_{ky} Y_k = -\rho D_k \frac{Y_k}{X_k} \frac{dX_k}{dy} - \frac{D_{Tk}}{T} \frac{dT}{dy} + \rho Y_k V_y^C, \quad (4)$$

where X_k is the mole fraction of species k , D_k is the diffusion coefficient of species k into the gas mixture, D_{Tk} is the thermal diffusion coefficient of species k , and the velocity correction ensuring mass conservation is

$$V_y^C = \sum_{k=1}^N \left(D_k \frac{Y_k}{X_k} \frac{dX_k}{dy} + \frac{D_{Tk}}{\rho T} \frac{dT}{dy} \right). \quad (5)$$

The transport equation for the gas temperature, T , can be expressed as

$$\rho C_p u_y \frac{dT}{dy} = \frac{d}{dy} \left(\lambda \frac{dT}{dy} \right) - \rho \frac{dT}{dy} \sum_{k=1}^N (C_{pk} V_{ky} Y_k) + \dot{\omega}_T + \dot{S}_e, \quad (6)$$

where C_p and C_{pk} denote the specific heat capacity at constant pressure of the gas mixture and of species k , respectively, λ is the thermal conductivity, and $\dot{\omega}_T$ and \dot{S}_e are source terms due to chemical reactions and exchange of energy between the liquid and gas phase, respectively.

The mixture fraction, ξ , is defined as a scalar satisfying the following transport equation

$$\rho u_y \frac{d\xi}{dy} = \frac{d}{dy} \left(\rho D_\xi \frac{d\xi}{dy} \right) + \dot{S}_v (1 - \xi), \quad (7)$$

where D_ξ is the diffusion coefficient assumed to be equal to $\lambda/(\rho C_p)$, for Lewis number $Le_\xi = \frac{\lambda}{\rho D_\xi C_p} = 1$. Equation (7) is an extension of the original work by Pitsch and Peters for gas flames [12], which avoids the inconsistencies arising from considering the same diffusion coefficients for all chemical species in the classical derivation of the transport equation of mixture fraction, but not in the chemical species transport equations.

A transport equation for the gradient of the mixture fraction

$$g_\xi = \frac{d\xi}{dy}, \quad (8)$$

can be obtained from the transport equation of the mixture fraction. Inserting Eq. (8) into Eq. (7) yields

$$\rho u_y g_\xi = \frac{d}{dy} (\rho D_\xi g_\xi) + \dot{S}_v (1 - \xi). \quad (9)$$

Note that the classical definition of the scalar dissipation rate of the mixture fraction is directly related to g_ξ

$$\chi = 2D_\xi g_\xi^2. \quad (10)$$

Despite this rather simple relation between both variables, Eq. (9) and its transformation into mixture fraction space are considerably simpler than previous formulations [4] directly obtained for χ . For the transformation of the governing equations presented above, the following change of coordinate from physical space into mixture fraction space is introduced

$$\frac{d(\cdot)}{dy} = g_\xi \frac{d(\cdot)}{d\xi}. \quad (11)$$

When Eq. (11) is applied to Eqs. (3) and (6), the spray flamelet equations for the mass fractions of chemical species and of the gas temperature yield

$$\underbrace{g_\xi^2 \rho \frac{D_\xi}{Le_k} \frac{d^2 Y_k}{d\xi^2}}_{I_{Y_k}} = \underbrace{-\dot{\omega}_k}_{II_{Y_k}} + \underbrace{\frac{dY_k}{d\xi} g_\xi \frac{d}{d\xi} \left(\rho D_\xi \left(\frac{Le_k - 1}{Le_k} \right) g_\xi \right)}_{III_{Y_k}} + \underbrace{g_\xi \frac{d(\tilde{V}_{k\xi} g_\xi)}{d\xi}}_{IV_{Y_k}} + \underbrace{\frac{dY_k}{d\xi} \dot{S}_v (1 - \xi) - \dot{S}_v (\delta_{kF} - Y_k)}_{IV_{Y_k}} \quad (12)$$

and

$$\underbrace{g_\xi^2 \rho D_\xi C_p \frac{d^2 T}{d\xi^2}}_{I_T} = \underbrace{-\dot{\omega}_T}_{II_T} - \underbrace{\frac{dT}{d\xi} g_\xi^2 \rho D_\xi \frac{dC_p}{d\xi} + g_\xi^2 \rho \frac{dT}{d\xi} \sum_{k=1}^N (C_{pk} V_{k\xi} Y_k)}_{III_T} + \underbrace{C_p \frac{dT}{d\xi} \dot{S}_v (1 - \xi) - \dot{S}_e}_{IV_T}, \quad (13)$$

respectively, where

$$V_{k\xi} = -\frac{D_k}{Y_k} \frac{dY_k}{d\xi} + \frac{\tilde{V}_{k\xi}}{\rho Y_k}, \quad (14)$$

and

$$\tilde{V}_{k\xi} = -\rho D_k \frac{Y_k}{\bar{W}} \frac{d\bar{W}}{d\xi} - \frac{D_{Tk}}{T} \frac{dT}{d\xi} + \rho Y_k \sum_{k'=1}^N \left(D_{k'} \frac{Y_{k'}}{X_{k'}} \frac{dX_{k'}}{d\xi} + \frac{D_{Tk'}}{\rho T} \frac{dT}{d\xi} \right), \quad (15)$$

with \bar{W} denoting the mean molecular weight of the gas mixture.

The spray flamelet equation for the gradient of the mixture fraction, the major objective of this work, can be obtained applying the operator $g_\xi \frac{d(\cdot)}{d\xi}$ to Eq. (9). This yields

$$g_\xi \frac{d(\rho u_y g_\xi)}{d\xi} = g_\xi \frac{d}{d\xi} \left(g_\xi \frac{d(\rho D_\xi g_\xi)}{d\xi} \right) + g_\xi \frac{d}{d\xi} \left(\dot{S}_v [1 - \xi] \right), \quad (16)$$

which can be transformed into

$$\underbrace{g_\xi^2 \rho D_\xi \frac{d^2 g_\xi}{d\xi^2}}_{I_{g_\xi}} = \underbrace{g_\xi \hat{a}}_{II_{g_\xi}} - \underbrace{g_\xi^3 \frac{d^2(\rho D_\xi)}{d\xi^2} - 2g_\xi^2 \frac{d(\rho D_\xi)}{d\xi} \frac{dg_\xi}{d\xi}}_{III_{g_\xi}} + \underbrace{\frac{dg_\xi}{d\xi} \dot{S}_v (1 - \xi) - g_\xi \frac{d}{d\xi} \left(\dot{S}_v [1 - \xi] \right)}_{IV_{g_\xi}}. \quad (17)$$

Term I_{g_ξ} corresponds to a diffusive term, whereas II_{g_ξ} is the only term balancing the equation in gas flames when the product ρD is assumed to be constant [6], which is equivalent to neglect term III_{g_ξ} . Finally, IV_{g_ξ} comprises evaporation-related effects. It is important to note that, provided the source terms \dot{S}_v and \dot{S}_e are known, the only unclosed term in the SFE is

$$\hat{a} = \frac{d(\rho u)}{dy} = g_\xi \frac{d(\rho u)}{d\xi}. \quad (18)$$

For the closure of this quantity, the stream-like function [10]

$$f(\xi) = \int_0^\xi \frac{u_T}{r} d\xi', \quad (19)$$

is used which can be inserted into the mass balance equation, Eq. (1), to obtain

$$2\rho f' + g_\xi \frac{d(\rho u_y)}{d\xi} = \dot{S}_v, \quad (20)$$

where Eq. (11) has been employed. After rearrangement and integration, Eq. (20) yields

$$u_y = \frac{1}{\rho} \left[\int_0^\xi \frac{\dot{S}_v - 2\rho f'}{g_\xi} d\xi^* + (\rho u_y)_{\xi=0} \right]. \quad (21)$$

Introducing Eqs. (19) and (21) into Eq. (2) yields

$$g_\xi \frac{d}{d\xi} (\mu g_\xi f'') = \left[\int_0^\xi \frac{\dot{S}_v - 2\rho f'}{g_\xi} d\xi^* + (\rho u_y)_{\xi=0} \right] g_\xi f'' + \rho (f')^2 - \rho_0 a^2 - \frac{\dot{S}_m}{r}, \quad (22)$$

where the Euler equation has been used to express dp/dr as a function of the outer flow velocity and the strain rate, a [10]. This approach is similar to the one introduced by Continillo and Sirignano [10] who have shown that the term $\frac{\dot{S}_m}{r}$ is independent of r and, therefore, Eq. (22) is one-dimensional in mixture fraction space and it can be solved to obtain f' , which can be then replaced in Eq. (20) to calculate \hat{a} as

$$\hat{a} = g_\xi \frac{d(\rho u_y)}{d\xi} = \dot{S}_v - 2\rho f'. \quad (23)$$

In the next section, the framework for the validation and the analysis of the SFE is presented.

Assessment Framework and Closure of the SFE

For the validation of the SFE, numerical simulations of steady axi-symmetric ethanol/air counterflow flames are performed. For this purpose, a two-dimensional Eulerian/Lagrangian formulation is adopted. Following Continillo and Sirignano [10], the gas equations are transferred into a one-dimensional system for the gas-phase equations by means of a similarity transformation as provided above and it is used as extended by Gutheil and Sirignano [11] for variable density and detailed transport and detailed chemical reactions. The present detailed chemical reaction mechanism for ethanol/air consists of 38 species and 337 elementary reactions [13]. Heating and evaporation of spherically symmetric single-component droplets in a mono-disperse spray are considered, where droplet motion is formulated in a Lagrangian way [10, 11] and evaporation is described by means of the Abramzon-Sirignano model [14].

In the following, three different counterflow flames are considered. First, a gas flame is simulated where a pure air stream injected from the left side of the configuration is directed against a pure gaseous ethanol stream injected from the right side, which is established as a base case (Flame A). This flame is then perturbed injecting a spray from the air side of the configuration, which consists of liquid fuel droplets of 20 μm of initial radius. Liquid fuel/air equivalence ratios of 0.2 and 0.8 are considered (calculated neglecting the gaseous fuel from the opposed stream) and the resulting flames are denoted as Flame B and Flame C, respectively. For all the simulations, the same gas phase conditions are employed with a strain rate of 55/s and an air inflow velocity of 0.75 m/s, both conditions evaluated at the air side of the configuration. The temperature at the boundaries is 300 K and, for the spray flames, the initial droplet velocity and temperature are equal to the gas phase conditions at the inlet. These conditions are selected because they systematically illustrate how the spray affects the gas flame structure, with particular emphasis on the effects of increasing the liquid fuel/air equivalence ratio. The present choice also assures that the spray flames under consideration do not exhibit a non-monotonic behavior of the mixture fraction as in previous studies, which allows solving the SFE in a mixture fraction space which extends from zero to unity. Additionally, these monotonic profiles of mixture fraction assure a unique correspondence of the gas temperature as well as the mass fractions, which facilitates projecting the counterflow solutions into the mixture fraction space for comparison and closure of the SFE.

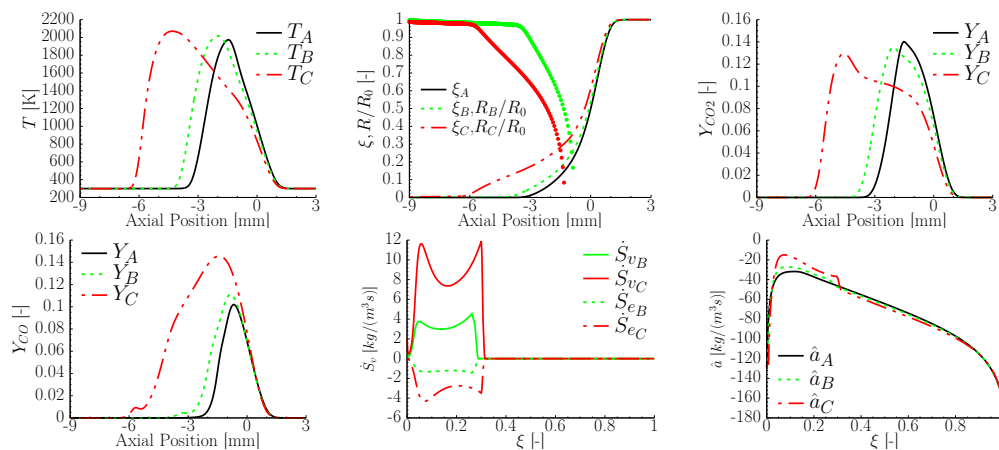


Figure 1. Gas temperature (top left), relative droplet radius (symbols) and mixture fraction (dashed lines) (top center), CO₂ mass fraction (top right), CO mass fraction (bottom left), mass evaporation rate (bottom center) and \hat{a} (bottom right) for Flames A, B and C.

The influence of varying the equivalence ratio in the outer flame structure is displayed in Fig. 1, where profiles of the gas temperature, the normalized droplet radius, CO₂ and CO mass fractions, as well as mass evaporation rates and the gradient of the product of gas velocity and gas density are shown for all flames. It can be observed that increasing the equivalence ratio generates a displacement of the peak of the gas temperature profile to the left side of the configuration (see Fig. 1 top left), which can be attributed to the higher amount of fuel available in that region. Moreover, the profile of the gas temperature becomes considerably wider as the equivalence ratio is increased. These effects promote evaporation and, consistently, they reduce the droplet penetration (see Fig. 1 top center) into the counterflow configuration. The displacement of the maximum temperature to the left side of the configuration also leads to a displacement of the peak of CO₂, as can be seen in Fig 1 (top right). This is an expected phenomenon, since the conversion of CO into CO₂ takes place mainly near to the high temperature region. Finally, a considerably increment of the total amount and the maximum value of CO is found when the equivalence ratio is increased, which is indicated by the peak value located at the low temperature region in the right side of the flame. This occurs since the energy available in that region is limited and, therefore, CO cannot be converted into CO₂ there.

The different strategies for the closure of the SFE are as follows. In particular, source terms that account for the mass, momentum, and energy exchange between the phases, \dot{S}_v , \dot{S}_m , and \dot{S}_e are unclosed quantities. For their closure, the projections into the mixture fraction space of the profiles obtained in the counterflow simulations presented in the previous section (see Fig. 1 (bottom center)) are employed. For the closure of $\hat{a} = d(\rho u_y)/dy$ in the SFE, the following three different approaches A1-A3 are considered:

- A1: The gas velocity obtained by means of Eq. (23) is employed to calculate \hat{a} . This approach is expected to fully recover the counterflow flame structures.
- A2: A constant value of $\hat{a} = \hat{a}_{st}$ is used, where \hat{a}_{st} is the value of \hat{a} at the stoichiometric value of the mixture fraction in the counterflow simulation. This value is chosen because there has been evidence that the conditions at stoichiometry are of importance for gas flames [1].
- A3: Again, a constant \hat{a} is adopted, which is assumed equal to its value at the left boundary (air side) of the counterflow configuration ($\hat{a} = \hat{a}_{-\infty}$). This approach is adopted because the value of \hat{a} at this location is typically known a priori, which is not the case in model A2.

Analysis of Fig. 1 (bottom right) shows that the difference between \hat{a}_{st} and $\hat{a}_{-\infty}$ increases with increased equivalence ratio, which is due to the corresponding reduction of \hat{a}_{st} explained above. Therefore, the best performance of A3 should occur for flame A, and this approach is expected to deteriorate when the spray gains in relevance.

In the remainder of this paper, the results obtained by solving the SFE with the three approaches A1, A2, and A3 will be denoted by subscripts "1", "2" and "3". In the next section, the numerical results will be compared and discussed.

Results and Discussion

A comparison of the different profiles of g_ξ using the different approaches A1, A2 and A3 is presented in Fig. 2 for the flames under consideration. Here, the subscript R corresponds to reference values obtained from the counterflow flames introduced in the previous section. An excellent agreement between the reference profiles and the profiles obtained by means of A1 is found for all cases, which confirms the validity of the spray flamelet equations and justifies the use of A1 as the reference case in the remainder of this section. A2 and A3, on the other hand, consistently lead to poor predictions of g_ξ through almost the entire flame structure. In particular, A2 results in an under-prediction, whereas A3 shows over-prediction. It is observed, however, that A2 performs better at low values of the mixture fraction where the reaction zone is located, and, therefore, this approach is expected to lead to better predictions of the chemical reaction zone compared to A3.

Regarding the influence of evaporation on the gradient of the mixture fraction, it is found that increasing the equivalence ratio tends to a reduction, which is explained by the more homogenous mixing that can be achieved when evaporation plays a role. This leads to a higher stability of the flame and is consistent with the higher strain rates required for extinction of spray flames in comparison with their gaseous counterpart [13].

Despite the big differences observed for the gradient of the mixture fraction, a comparison of the gas temperature profiles obtained by the different approaches reveals a better agreement for flames A, B, and C (see Fig. 3), where A2 performs considerably better than A3. Since g_ξ is well reproduced for A2 in the low mixture fraction region, the good temperature prediction obtained in this zone with this approach is not surprising. For A3, however, a slight under-prediction of the gas temperature is observed in this region, which is due to the higher values of g_ξ that

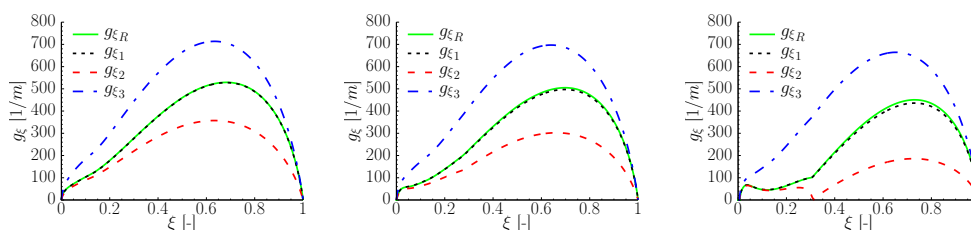


Figure 2. Profiles of g_ξ for Flame A (left), Flame B (center) and Flame C (right).

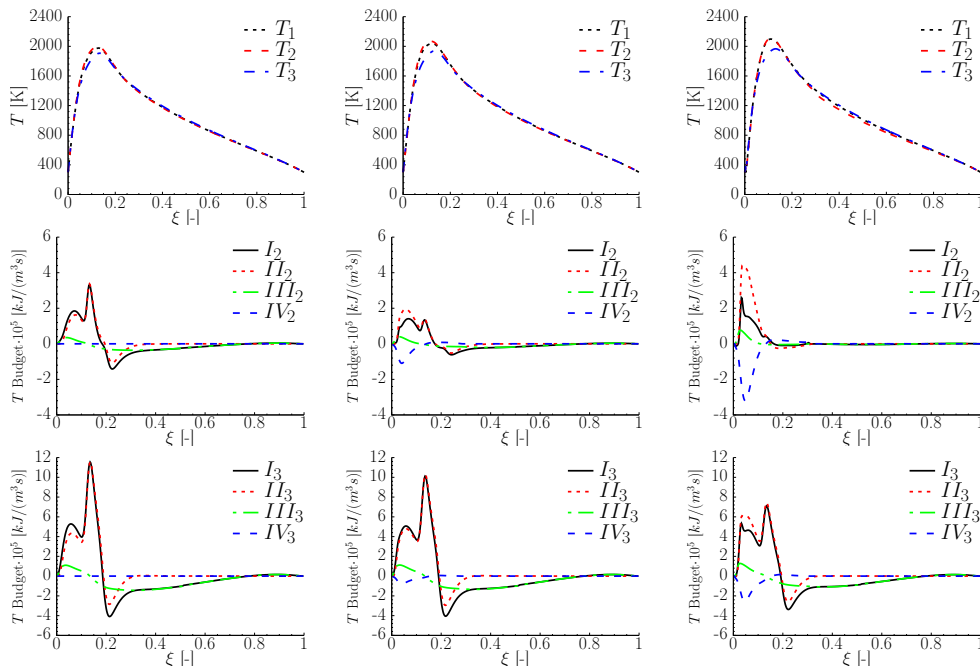


Figure 3. Profiles of gas temperature (top), budget of terms in temperature flamelet equation using A2 (center) and using A3 (bottom) for Flame A (left), Flame B (center) and Flame C (right).

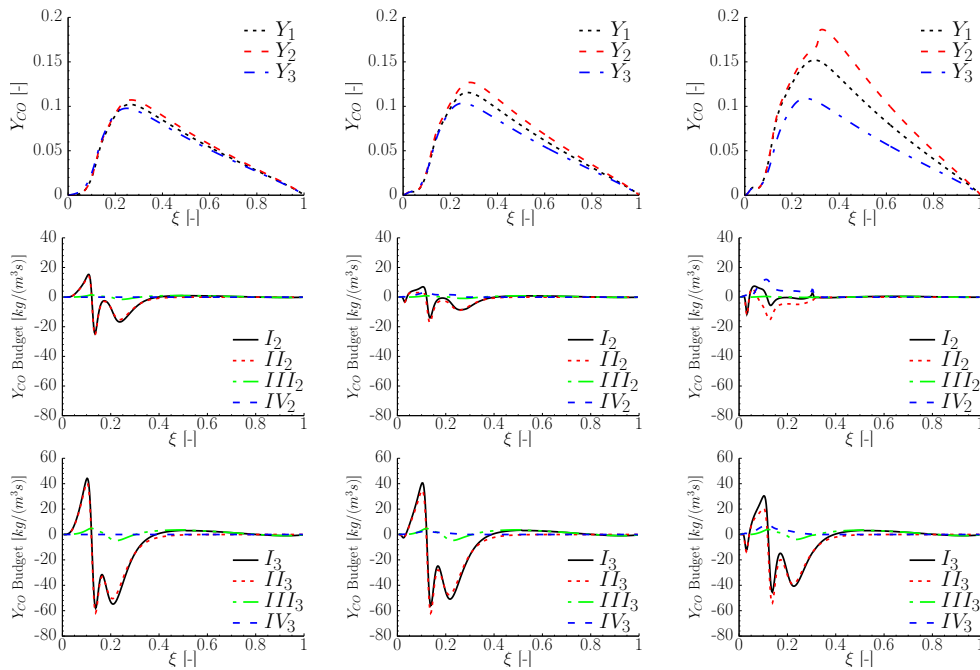


Figure 4. CO profiles (top), budget of terms in CO-flamelet equation using A2 (center) and using A3 (bottom) for Flame A (left), Flame B (center) and Flame C (right).

are obtained in this zone. Specifically, this phenomenon occurs because an over-prediction of the gradient of the mixture fraction implies a higher diffusion of energy from the reaction zone to the surroundings and leads therefore to a reduction of the local gas temperature. This is consistent with the classical gas flamelet theory [1], which explains how gas temperature is reduced when the value of the scalar dissipation rate at the stoichiometric point is increased.

Regarding the physical processes dominating the temperature flamelet equation, major differences are found for A2 and A3. For A2, it can be clearly seen, cf. Fig. 3, how evaporation reduces diffusion and increases the value and relative importance of term IV. This is especially notorious for Flame C, and consistent with previous findings [3]. For A3, the dominant physical processes are not changed by evaporation and the energy source due to chemical reaction is always mainly balanced by diffusion. This rather counterintuitive result is explained by the over-prediction of the contribution of the diffusive term obtained with A3, which makes term IV to appear small in comparison, reducing the relative importance of evaporation effects on the flamelet equation for the gas temperature. This result

shows that, even when acceptable gas temperature predictions are obtained by means of A3, a poor description of the involved physics is achieved with this approach.

Finally, Fig. 4 shows the profiles of the mass fraction of CO for the flames under consideration. It is found that good predictions are obtained for Flame A, whereas still acceptable values are calculated for Flame B. For Flames C, however, only poor predictions are obtained. To understand the reason for this, it is again necessary to analyze the budgets of the CO flamelet equations, which are also presented in Fig. 4 for A2 (center) and A3 (bottom), respectively. It can be seen that chemical reactions take place in an extended zone between values of the mixture fraction of zero and 0.4, which extends well beyond the region in which g_ξ may be properly reproduced. The poor prediction even worsens when the equivalence ratio is increased, since the relative error with which the gradient of the mixture fraction is predicted, increases with the equivalence ratio. Finally, for the chemical species CO, the underlying physical and chemical processes taking place simultaneously are not properly identified using A3, confirming the superiority of A2 over A3.

Conclusions

The use of the gradient of the mixture fraction, $g_\xi = d\xi/dy$, has been proposed for closing the scalar dissipation rate in the spray flamelet equations (SFE), and a transport equation for this new quantity has been derived and transformed into the mixture fraction space. For this purpose, the SFE have been re-derived in terms of g_ξ . These equations are validated in the context of several laminar ethanol/air counterflow flame structures. In particular, a pure ethanol/air gas flame (Flame A) was used as a base case and three additional flames were generated by perturbing the air side with a mono-disperse spray and increasing the equivalence ratio at the air side of the configuration (Flames B to D). After this, two additional flames were generated by increasing the initial droplet sizes of the monodisperse spray (Flames E and F).

In the newly proposed SFE, two types of unclosed quantities are found: The spatial gradient of the product of gas density and velocity $\hat{a} = d(\rho u_y)/dy$ as well as evaporation-related source terms. Two different approaches were proposed for the closure of \hat{a} : Introducing a stream-like function and using the global mass and axial momentum balance equations to derive an expression for it (Approach A1) and assuming a constant value for \hat{a} . Specifically, it was proposed to use the value of \hat{a}_{st} at stoichiometric mixture (Approach A2) and at the air side of the counterflow configuration $\hat{a}_{-\infty}$ (Approach A3). For the closure of the evaporation-related source terms, profiles obtained from the numerical simulations in physical space were employed. The different closure alternatives were evaluated in terms of their capability of predicting the profile of g_ξ and the spray flamelet structure of the different reference counterflow flames.

The results show that approach A1 can perfectly reproduce both, the spray flamelet structure and the contribution of the different terms appearing in the SFE for all flames under study, which clearly highlights its advantages over A2 and A3. Approach A2 can adequately capture the relative importance of the main physical phenomena occurring in the reference counterflow flames, even when the flame structure itself is not always well-predicted by this approach. Particularly, A2 fails for situations in which evaporation takes place far away from the main reaction zone. Finally, A3 was found to be incapable of properly capturing the influence of evaporation and generally led to inappropriate predictions.

The present results contribute towards the formulation of a comprehensive and self-contained spray flamelet theory. However, there is still a need for proper closure of the evaporation-related source terms appearing in the SFE in mixture fraction space, which will be the focus of future work.

Acknowledgments

The authors thank CONICYT (Chile) for financial support through FONDECYT Grant 11171020. EG acknowledges financial support of the German Research Foundation (DFG) through SPP 1980, grant GU 255/13-1.

References

- [1] Peters, N., 1984, *Progress in Energy and Combustion Science*, 10 (3), pp. 319-339
- [2] Luo, K., Fan J., Cen, K., 2013, *Fuel*, 103, pp. 1154-1157
- [3] Olguin, H., Gutheil, E., 2014, *Combustion and Flame*, 161 (4), pp. 987-996
- [4] Olguin, H., Gutheil, E., 2015, *Zeitschrift für Physikalische Chemie*, 229 (4), pp. 461-482
- [5] Franzelli, B., Vié, A., Ihme, M., 2015, *Combustion Theory and Modelling*, 19 (6), pp. 773-806
- [6] Hasse, C., Peters, N., 2005, *Proceedings of the Combustion Institute*, 30 (2), pp. 2755-2762
- [7] Scholtissek, A., Dietzsch, F., Gauding, M., Hasse, C., 2017, *Combustion and Flame*, 175, pp. 243-258
- [8] Gomet, L., Robin, V., Mura, A., 2014, *Acta Astronautica*, 94 (1), pp. 184-197
- [9] Scholtissek, A., Domingo, P., Vervisch, L., Hasse, C., 2018, *Proc. Combust. Inst.*, 37 (2), pp. 1529-1536
- [10] Continillo, G., Sirignano, W., 1990, *Combustion and Flame*, 81 (3), pp. 325-340
- [11] Gutheil, E., Sirignano, W., 1998, *Combustion and Flame*, 113 (1), pp. 92-105
- [12] Pitsch, H., Peters, N., 1998, *Combustion and Flame*, 114 (1-2), pp. 26-40
- [13] Gutheil, E., 2001, *Combustion Theory and Modelling*, 5(2), pp. 131-145
- [14] Abramzon, B., Sirignano, W., 1989, *International Journal of Heat and Mass Transfer*, 32 (9), pp. 1605-1618